Two-dimensional dissipative gap solitons

Hidetsugu Sakaguchi[1] and Boris A. Malomed[2]
[1]*Department of Applied Science for Electronics and Materials, Interdisciplinary Graduate School of Engineering Sciences, Kyushu University, Kasuga, Fukuoka 816-8580, Japan*
[2]*Department of Physical Electronics, School of Electrical Engineering, Faculty of Engineering, Tel Aviv University, Tel Aviv 69978, Israel*
(Received 20 May 2009; published 26 August 2009)

We introduce a model which integrates the complex Ginzburg-Landau equation in two dimensions (2Ds) with the linear-cubic-quintic combination of loss and gain terms, self-defocusing nonlinearity, and a periodic potential. In this system, stable 2D *dissipative gap solitons* (DGSs) are constructed, both fundamental and vortical ones. The soliton families belong to the first finite band gap of the system's linear spectrum. The solutions are obtained in a numerical form and also by means of an analytical approximation, which combines the variational description of the shape of the fundamental and vortical solitons and the balance equation for their total power. The analytical results agree with numerical findings. The model may be implemented as a laser medium in a bulk self-defocusing optical waveguide equipped with a transverse 2D grating, the predicted DGSs representing spatial solitons in this setting.

DOI: 10.1103/PhysRevE.80.026606 PACS number(s): 05.45.Yv, 03.75.Lm, 42.65.Tg

I. INTRODUCTION AND THE MODEL

Equations of the complex Ginzburg-Landau (CGL) type are universal asymptotic models to describe the nonlinear pattern formation in dissipative media [1]. They also find direct (rather than asymptotically derived) realizations in nonlinear optics as models of laser cavities [2]. Objects of fundamental interest predicted by the CGL equations are solitary pulses (SPs), alias dissipative solitons. They represent, in particular, temporal pulses generated by fiber lasers [2–4] and, in an altogether different physical context, patches of traveling-wave thermal convection in narrow channels [5].

The simplest CGL equation is based on the cubic nonlinearity. Exact one-dimensional (1D) SP solutions are known in that case [6], but they are unstable, as the respective equation includes the linear gain, compensating the cubic loss, which destabilizes the zero background around the pulses and leads to the formation of a chaotic "gas" of SPs [7]. A well-known modified equation that can support *stable* SPs includes a combination of linear and quintic loss terms and cubic gain; therefore, it is called the cubic-quintic (CQ) CGL equation. This equation was introduced [in the two-dimensional (2D) form] in Ref. [8]. Stable SP solutions to the 1D version of the CQ-CGL equation were first predicted by means of an analytical approximation based on the power-balance analysis for solitons of the nonlinear Schrödinger (NLS) equation [9]. Then, these solutions were explored in detail by means of numerical methods [10]. More general models, such as linearly coupled systems of CQ-CGL equations [11] and the complex Swift-Hohenberg equation with the CQ nonlinearity [12], were introduced too.

In addition to the solitons of the NLS type, a generic species of solitary waves in conservative media is represented by gap solitons. They are well known in nonlinear optics, as temporal solitons in fiber Bragg gratings, and in Bose-Einstein condensates (BECs) with repulsion between atoms, which are loaded into in optical-lattice trapping potentials. A fundamental feature, from which the name of the gap soliton derives, is that its wave number (in terms of optical models) must belong to a finite band gap induced by the effective periodic potential. In the context of both the fiber gratings [13–15] and matter waves (BEC) [16,17], gap solitons were predicted theoretically, including 2D gap solitons in BEC [18,19], and 2D solitons with embedded vorticity [20]. The creation of optical and matter-wave gap solitons was reported in the 1D geometry—in short fiber gratings [21], and in the condensate loaded into an optical lattice combined with a strong transverse trap [22], respectively.

A generalization of the above concepts, aiming to predict dissipative gap solitons (DGSs), was proposed recently [23]. The respective version of the CGL equation combines a periodic potential and the set of the CQ loss and gain terms,

$$i\frac{\partial \psi}{\partial t} = -\frac{1}{2}\frac{\partial^2 \psi}{\partial x^2} + |\psi|^2\psi - A\cos\left[2q_0\left(x-\frac{L}{2}\right)\right]\psi + i\epsilon(-\gamma_1 + \gamma_2|\psi|^2 - \gamma_3|\psi|^4)\psi. \quad (1)$$

Here, ψ may be considered as the local amplitude of the electromagnetic wave (in the case of an optical model), A and π/q_0 are the strength and period of the potential ($x=L/2$ is the midpoint of the system), and coefficients $\epsilon\gamma_1$, $\epsilon\gamma_3$, and $\epsilon\gamma_2$ represent the linear and quintic dissipation and cubic gain, respectively. The conservative cubic term in Eq. (1) is defined with the self-defocusing sign, which is relevant to gap solitons.

A physical realization of Eq. (1) pertains to a planar self-defocusing optical waveguide, in which the periodic potential may be induced by a transverse grating (periodic modulation of the refractive index). In particular, a self-defocusing nonlinearity, in the combination with photoinduced transverse lattices, can be implemented in photorefractive crystals [24]. As concerns the CQ loss/gain terms, they may actually represent a combination of the linear amplification and saturable absorption, which is a common setting in laser cavities [4,25]. In terms of this interpretation, variable t in Eq. (1) designates the propagation distance, while x is the transverse

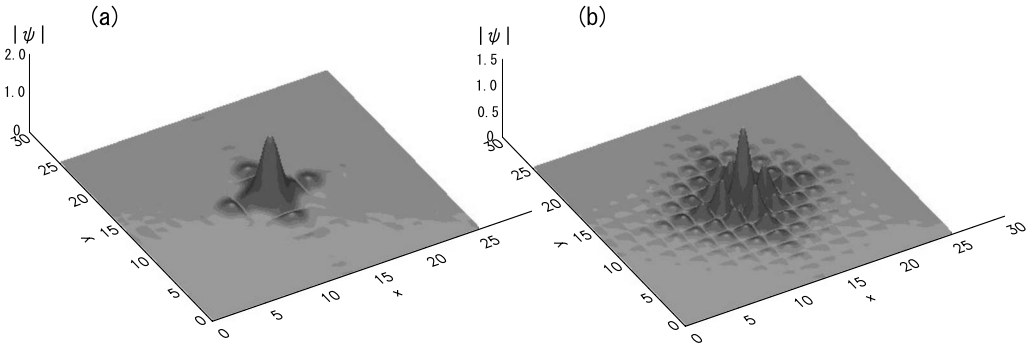

FIG. 1. Numerically generated profiles of stable fundamental tightly and loosely bound 2D gap solitons $|\psi(x,y)|$ found, respectively, at (a) $q_0=1$, and at (b) $q_0=1.75$. Other coefficients are $\gamma_1=0.5$, $\gamma_2=2$, $\gamma_3=1$, $\epsilon=0.05$, and $A=2$.

coordinate [hence, the SP solutions to be produced by Eq. (1) will be spatial solitons [23]]. It is also relevant to mention the model combining the standard fiber-Bragg-grading part and the CQ combination of dissipative terms, in which temporal DGSs were investigated [26], including interactions between them [27].

The analysis reported in Ref. [23] revealed, by means of approximate analytical and direct numerical methods, the existence of three families of stable DGSs in the first finite band gap of the respective linear spectrum: loosely and tightly bound static solitons and a family of breathers between them. All the families were found close to the border between the finite band gap and Bloch band separating it from the semi-infinite gap, the tightly and loosely bound DGSs being located in spectral regions where the Bloch band is, respectively, very narrow or relatively wide. Stable dark solitons were also found in the model, and the mobility of dark and loosely bound bright solitons was demonstrated in it (collisions between mobile solitons are quasielastic).

The objective of the present work is to introduce fundamental and vortical DGSs in *two dimensions*. To this end, we consider the 2D extension of Eq. (1),

$$i\frac{\partial\psi}{\partial t}=-\frac{1}{2}\nabla^2\psi+|\psi|^2\psi-A\left\{\cos\left[2q_0\left(x-\frac{L}{2}\right)\right]+\cos\left[2q_0\left(y-\frac{L}{2}\right)\right]\right\}\psi+i\epsilon(-\gamma_1+\gamma_2|\psi|^2-\gamma_3|\psi|^4)\psi. \tag{2}$$

This equation may be interpreted as governing the propagation of electromagnetic waves in a bulk medium with the self-defocusing nonlinearity and other ingredients included in Eq. (1), assuming that the potential periodic in x and y is induced by the 2D transverse grating, with t again having the meaning of the propagation distance. In Sec. II, solutions for fundamental gap solitons are found, in parallel, in a numerical form [as attractors of Eq. (2)], and by means of an analytical approach, which combines a variational approximation (VA) for the shape of the solitons and the balance equation for their total power. In terms of the corresponding linearized equation, the soliton family belongs to the first finite band gap. Further, in Sec. III we report the existence of stable vortex solitons (with topological charge 1) built as complexes of four peaks, with the phase shift of $\pi/2$ between adjacent ones, and an empty site in the center (*rhombus-shaped* vortices [28], alias *on-site* ones). The vortex solitons are constructed as stable numerical solutions and are also obtained by means of the analytical approximation. Thus, the results reported in this work predict the existence of stable spatial solitons, both fundamental and vortical ones, in laser cavities based on self-defocusing bulk media with transverse gratings.

II. FUNDAMENTAL SOLITONS

Stable solutions to Eq. (2) in the form of 2D fundamental (zero-vorticity) solitons can be readily found, in the first finite band gap, as *attractors* of the CGL equation, by dint of direct simulations starting with an appropriate initial configuration. Typical examples of such *tightly* and *loosely* localized gap solitons are displayed in Fig. 1. The 2D solitons become looser with the decrease in the lattice period π/q_0 as the soliton spreads over a larger number of lattice cells.

The shape of the fundamental solitons is determined by the equation for complex function $\phi(x,y)$ obtained by the substitution of $\psi(x,y,t)=e^{-i\mu t}\phi(x,y)$ in Eq. (2), where $-\mu$ is the soliton's propagation constant, in terms of the optical model. To approximate the soliton's shape in an analytical form, we start with the equation for $\phi(x,y)$ without the dissipative terms ($\epsilon=0$). The latter equation can be derived from Lagrangian $\Lambda=\int\int\mathcal{L}dxdy$, with density

$$\mathcal{L}=\mu|\phi|^2-\frac{1}{2}(|\nabla\phi|^2+|\phi|^4)+A\left\{\cos\left[2q_0\left(x-\frac{L}{2}\right)\right]+\cos\left[2q_0\left(y-\frac{L}{2}\right)\right]\right\}|\phi|^2. \tag{3}$$

In this approximation, $\phi(x,y)$ may be assumed real, therefore, following the lines of Refs. [29,30], we adopt the variational ansatz as

$$\phi=B\exp\left\{-\frac{a}{2}\left[\left(x-\frac{L}{2}\right)^2+\left(y-\frac{L}{2}\right)^2\right]\right\}\times\cos\left[q\left(x-\frac{L}{2}\right)\right]\cos\left[q\left(y-\frac{L}{2}\right)\right], \tag{4}$$

where amplitude B and width a^{-1} are free parameters, the norm of ansatz (4) being

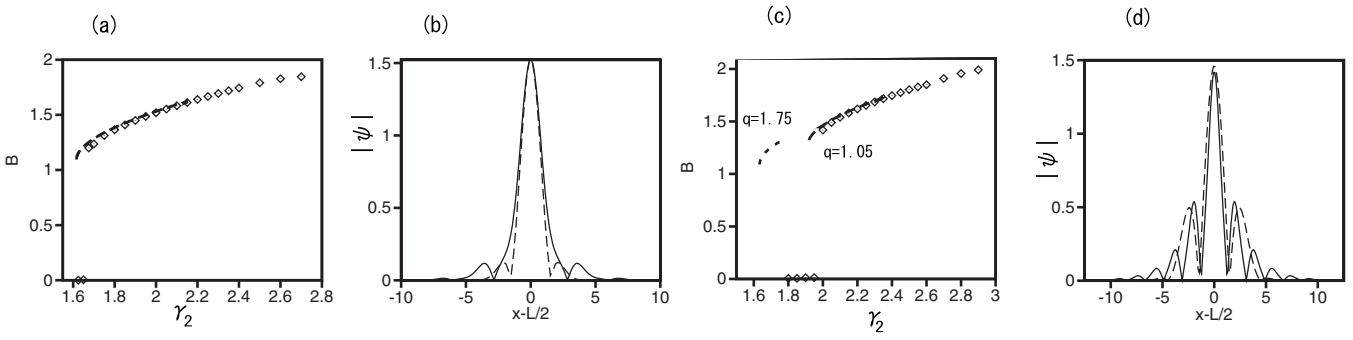

FIG. 2. (a) Numerically found amplitude B of tightly bound dissipative gap solitons (diamonds) and the respective analytical prediction (lines) versus cubic gain γ_2. Other coefficients are $A=2$, $q_0=1$, $\epsilon=0.05$, $\gamma_1=0.5$, $\gamma_3=1$, and $q=q_0=1$. (b) The comparison of the numerically found and analytically predicted cross sections of the soliton profiles $|\psi(x,y=L/2)|$ for $q=q_0=1$, $\epsilon=0.05$, $\gamma_1=0.5$, $\gamma_3=1$, and $\gamma_2=2$ (the case of relatively tightly bound profiles). (c) Numerically found amplitude B of loosely bound dissipative gap solitons and the respective analytical prediction obtained with fitting parameter $q=q_0=1.75$ or $q=0.6q_0=1.05$, versus cubic gain γ_2, for $q_0=1.75$. (d) The comparison of the numerically found and analytically predicted cross sections of loosely bound soliton profiles for $q_0=1.75$, with the choice of $q=1.05$.

$$N \equiv \int\int |\phi(x,y)|^2 dxdy = \pi B^2 (4a)^{-1} (1 + e^{-q^2/a})^2 \quad (5)$$

(in terms of the laser-cavity model, N is proportional to the total power of the light beam).

Ansatz (4) implies that constant q may be different from q_0 in Eq. (2). In fact, for the description of tightly bound (strongly localized) solitons, it will be sufficient to fix $q=q_0$, which is not surprising, as the mismatch between the periodic functions in the ansatz and the periodicity of the potential, accounted for by $q \neq q_0$, is not crucially important for the well-localized wave forms. On the other hand, applying the VA to loosely bound (weakly localized) solitons, we will treat q not as a variational parameter but rather as a "phenomenological" fitting constant. We also tried an extended version of the VA, which subjected q to variation too, but it yielded essentially less accurate results. This conclusion may be explained by the difficulty in approximating the complex shape of loosely bound solitons by a simple ansatz. Similar situation are known in other applications of VA to the description of complicated wave patterns, where some parameters should be still treated as variational ones, while others are reserved for direct fitting (cf., e.g., Ref. [31]).

The substitution of ansatz (4) into Lagrangian density (3) and the integration yield the effective Lagrangian expressed in terms of N, a, and q,

$$\Lambda_{\rm eff} = N\left\{ \mu - \frac{ae^{-q^2/a} + a + 2q^2}{2(1+e^{-q^2/a})} + A\frac{e^{-(q_0-q)^2/a} + e^{-(q_0+q)^2/a} + 2e^{-q_0^2/a}}{1+e^{-q^2/a}} - \frac{Na}{16\pi}\frac{[1+e^{q^2/(2a)}]^4[e^{-2q^2/a} - 2e^{-3q^2/(2a)} + 3e^{-q^2/a}]^2}{(1+e^{-q^2/a})^4} \right\}. \quad (6)$$

Variational equation $\partial\Lambda/\partial a=0$ for fixed q determines a as a function of N (as said above, q is not a variational parameter; hence, we do not add equation $\partial\Lambda/\partial q=0$).

At the next stage of the analysis, we restore the dissipative terms in Eq. (2) and, treating them as small perturbations, derive a straightforward evolution equation for the total norm,

$$\frac{dN}{dt} = 2\epsilon(-\gamma_1 N + \gamma_2 N_2 - \gamma_3 N_3), \quad (7)$$

where the following coefficients were calculated as per ansatz (4):

$$N_2 = \int\int |\psi|^4 dxdy = \frac{\pi B^4}{128a} e^{-4q^2/a}[1+e^{q^2/(2a)}]^4 \times [1 - 2e^{q^2/(2a)} + 3e^{q^2/a}]^2, \quad (8)$$

$$N_3 = \int\int |\psi|^6 dxdy = \frac{\pi B^6}{3072a}[10 + e^{-3q^2/a} + 6e^{-4q^2/(3a)} + 15e^{-q^2/(3a)}]^2. \quad (9)$$

According to Eq. (7), the balance condition for the norm in the stationary state $dN/dt=0$ yields relation

$$\gamma_2 N_2 = \gamma_1 N + \gamma_3 N_3. \quad (10)$$

Figure 2(a) displays the amplitude of the DGS, B for $q_0=1$, versus cubic gain γ_2, as predicted by the analytical approximation with $q=q_0$, i.e., obtained from a numerical solution of Eqs. (5) and (10), along with the same dependence generated by direct simulations. It is seen that the analytical approximation provides good overall accuracy for the solitons which feature a (relatively) tightly bound shape (therefore, it is sufficient to set $q=q_0$, i.e., one does not need an extra fitting parameter in this case), although the approximation predicts the existence of the solitons at $\gamma_2 \leq 2.15$, while the direct simulations yield stable DGSs at $\gamma_2 \leq 2.7$. For $\gamma_2 > 2.7$, the simulations produce delocalized solutions, as the

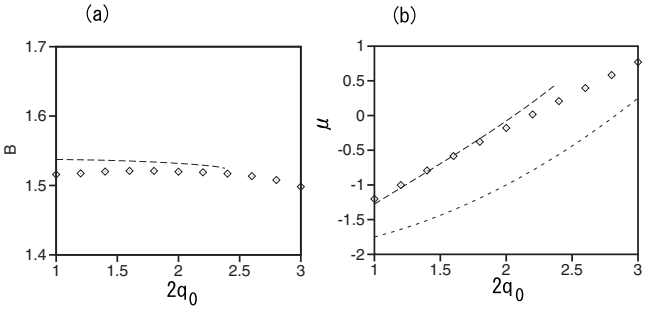

FIG. 3. (a) Amplitude B and (b) propagation constant μ of fundamental solitons versus the grating's wave number $2q_0$ for $A=2$ and $\epsilon=0.05$, $\gamma_1=0.5$, $\gamma_2=2$, $\gamma_3=1$. Diamonds and bold dashed curves show, respectively, direct numerical results and predictions of the straightforward analytical approximation obtained with $q=q_0$ (no fitting). The thin dashed curve in (b) is the lower border of the first finite band gap [as found with $\epsilon=0$, i.e., in the conservative version of Eq. (2)], to which the soliton family belongs.

loss terms cannot compensate the gain in that region. The trend to underestimating the existence area for the DGS by the analytical approximation is generic, persisting throughout the parameter space.

For the same case of $q=q_0=1$, Fig. 2(b) displays comparison of the soliton's cross-section profile $|\psi(x,y=L/2)|$ and the respective analytical approximation. For given values of the parameters, the latter one is $|\psi(x,y=L/2)|=1.53e^{-0.413x^2}\cos(x-L/2)$ [see Eq. (4)]. It is seen that the analytically predicted and numerically found profiles overlap well near the soliton's center, but points at which $\phi(x)$ crosses zero are shifted.

Figure 2(c) displays the amplitude of *loosely bound solitons* versus γ_2, for $q_0=1.75$. The plot shows both the straightforward prediction of the analytical approximation obtained with $q=q_0=1.75$ and its "phenomenologically" adjusted modification provided by choosing $q=0.6q_0=1.05$. In the direct numerical simulations, the respective DGSs exist for $1.95<\gamma_2<2.95$, while the analytical solution with $q=q_0=1.75$ exists in the region of $1.64<\gamma_2<1.75$, which does not overlap at all with its numerical counterpart. However, choosing the fitting parameter to be $q=1.05$ allows us to fit the region of the existence of the analytical solutions to the numerical one fairly well. Accordingly, the comparison of the numerically found soliton's cross-section profile $|\psi(x,y=L/2)|$ and the respective analytical approximation with $q=1.05$, which is $|\psi(x,y=L/2)|=1.46e^{-0.151x^2}\cos 1.05(x-L/2)$ in the present case, is displayed in Fig. 2(d).

Figure 3 shows another set of global characteristics of the DGS family, viz., the amplitude and propagation constant (B and μ) versus the grating's wave number, as found in the numerical and analytical forms. In particular, panel 3(b) clearly shows that the entire DGS family falls into the first finite band gap of the underlying linear spectrum. The figure also demonstrates the same trend as mentioned above, namely, that the analytical approximation, while predicting generally correct characteristics of the soliton family, underestimates its existence range: it does not yield solutions for $q_0>1.2$, while the direct simulations converge to DGSs up to $q=1.85$ (numerically found solutions get delocalized at $q_0>1.85$).

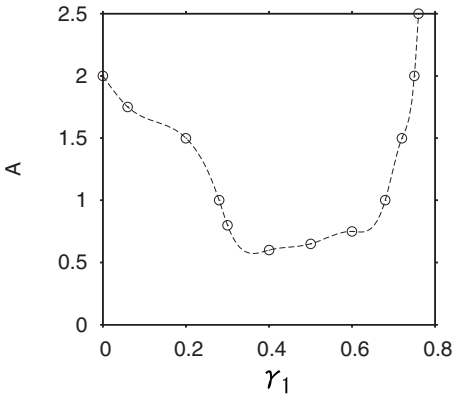

FIG. 4. Stable fundamental gap solitons exist above the continuous curve in the (γ_1,A) plane. Other parameters are $\gamma_2=2$, $\gamma_3=1$, $\epsilon=0.05$, and $q_0=1$.

The existence range for the stable DGSs in the plane of parameters, which control the linear part of the model, viz., loss coefficient γ_1 and grating strength A, as found from the numerical results, is displayed in Fig. 4. To the right of the border shown in Fig. 4 (i.e., if the linear attenuation is too strong), numerical solutions decay to zero, while to the left of the border (if the attenuation is too weak) the solution undergoes a delocalization transition. It is relevant to mention that unlike DGSs in the 1D counterpart of the present model [23], no 2D soliton was found to be mobile [the application of the *kick*, i.e., multiplication by $\exp(iKx)$, fails to set any 2D soliton in persistent motion].

III. SOLITARY VORTICES

We have also found dissipative gap vortex solitons with topological charge 1. To generate the vortex soliton, we have performed numerical simulation of Eq. (2) starting with the initial configuration,

$$\psi(x,y)=B\left[\left(x-\frac{L}{2}\right)+i\left(y-\frac{L}{2}\right)\right]\exp\left\{-\left(\frac{a}{2}\right)\left[\left(x-\frac{L}{2}\right)^2+\left(y-\frac{L}{2}\right)^2\right]\right\}\cos\left[q\left(x-\frac{L}{2}\right)\right]\cos\left[q\left(y-\frac{L}{2}\right)\right], \tag{11}$$

where the pre-exponential multiplier accounts for topological charge 1 of the vortex. Typical examples of stable vortices are displayed in Fig. 5, at the same values of parameters for which stable fundamental solitons were shown in Fig. 1. Figure 5(a) displays a rhombus-type vortex soliton for $q_0=1$, which is composed of four peaks with the phase shift of $\pi/2$ between adjacent ones. Figure 5(b) displays a more loosely bound vortex soliton, for $q_0=1.6$. The solitary vortices feature a transition from the tightly bound shape to the loose one with the decrease in the period of the underlying grating π/q_0. In any case, main peaks which form vortices are located, approximately, at $(x,y)=(L/2+\pi/q_0,L/2)$, $(L/2-\pi/q_0,L/2)$, $(L/2,L/2-\pi/q_0)$ and $(L/2,L/2+\pi/q_0)$. The

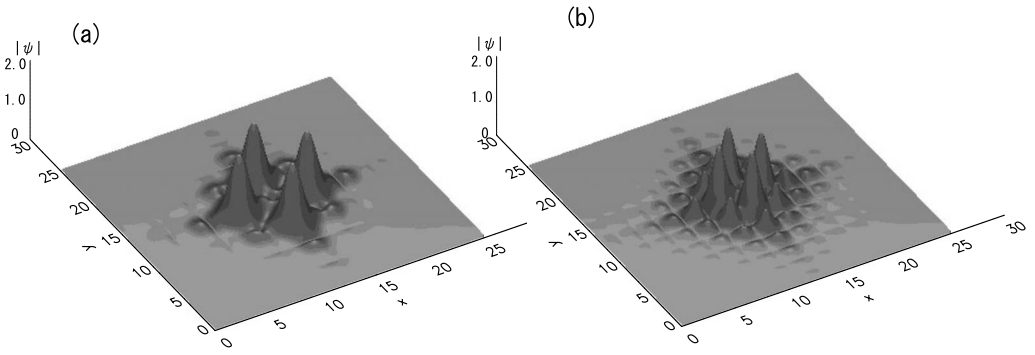

FIG. 5. Profiles of vortex gap solitons $|\psi(x,y)|$ produced by the direct simulations at (a) $q_0=1$ and (b) 1.6 for $\gamma_1=0.5$, $\gamma_2=2$, $\gamma_3=1$, $\epsilon=0.05$, and $A=2$.

vortex slowly becomes delocalized at still larger values of q_0, for instance, at $q_0=1.75$, if other parameters are fixed as in Fig. 5.

Getting back to the example of a tightly bound vortex obtained at $q_0=1$, which is built of the four peaks that are well localized around four potential minima $(x,y)=(L/2+\pi,L/2)$, $(L/2-\pi,L/2)$, $(L/2,L/2+\pi)$ and $(L/2,L/2-\pi)$, one may approximate each peak by ansatz (4) with $q=q_0$. Then, the entire vortex may be approximated as

$$\begin{aligned}\phi(x,y) = B\cos(x-L/2)\cos(y-L/2)\\ \times\{\exp[-a/2\{(x-L/2-\pi)^2+(y-L/2)^2\}]\\ + i\exp[-a/2\{(x-L/2)^2+(y-L/2-\pi)^2\}]\\ -\exp[-a/2\{(x-L/2+\pi)^2+(y-L/2)^2\}]\\ - i\exp[-a/2\{(x-L/2)^2+(y-L/2+\pi)^2\ ]\},\end{aligned} \tag{12}$$

where B and a are taken as predicted by the analytical approximation for the fundamental soliton.

Figure 6(a) shows the dependence of the vortex' amplitude on the cubic-gain coefficient γ_2 as found from the direct simulations for $q_0=1$, i.e., for the family of relatively tightly bound vortices. The dashed curve in Fig. 6(a) represents the corresponding analytical approximation for B in expression (12), which is found to agree with the numerical results. Further, Fig. 6(b) displays a typical example of the numerically and analytically found cross-section profiles of the tightly bound vortex, which also demonstrates good agreement between both [the dashed curve is $|\psi(x)|=1.532|\cos(x-L/2)[\exp\{-0.413(x-L/2-\pi)^2\}-\exp\{-0.413\times(x-L/2+\pi)^2\}]|$, as per Eq. (12)].

Proceeding to loosely bound vortices, Fig. 6(c) shows the dependence of the vortex' amplitude on γ_2 for $q_0=1.6$. The dashed curve in the same panel represents the respective analytical approximation for B adjusted by choosing $q=0.7q_0=1.12$ in ansatz (4). Further, Fig. 6(d) displays a typical example of the numerically and analytically found cross-section profiles of the vortex, also for $q_0=1.6$ and $q=0.7q_0=1.12$. The dashed (analytical) profile corresponds to $|\psi(x)|=B|\cos[q(x-L/2-\pi/q_0)]\exp[-(a/2)(x-L/2-\pi/q_0)^2]-\cos[q(x-L/2+\pi/q_0)]\exp[-(a/2)(x-L/2+\pi/q_0)^2]|$, where $B=1.461$ and $a=0.339$ are values predicted by the analytical approximation for the fundamental DGS. Good agreement between both profiles is observed.

IV. CONCLUSION

In this work, we have introduced a model combining the CGL equation in two dimensions with the CQ (cubic-quintic) combination of gain and loss terms, self-defocusing nonlinearity, and the 2D periodic potential. The model gives rise to stable DGSs (dissipative gap solitons), both fundamental and vortical ones. The DGS families were found in numerical

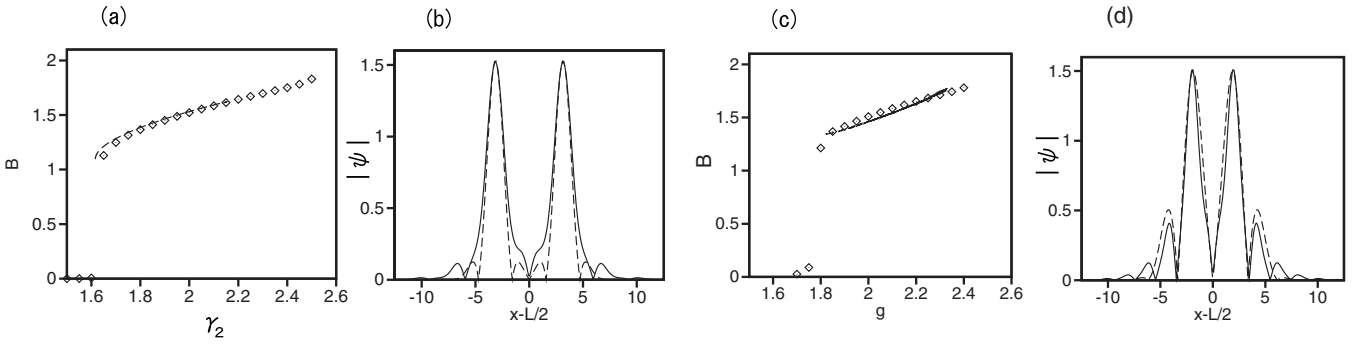

FIG. 6. (a) The same as in Fig. 2(a) (at the same values of parameters) but for the amplitude of the rhombus-shaped vortex. (b) The same as in Fig. 2(b) but for the cross-section profiles of the vortex. (c) The numerically found vortex' amplitude for $q_0=1.6$ and the respective analytical approximation (the dashed line) adjusted by choosing $q=0.7q_0=1.12$. (d) The same as in (b) but for $q_0=1.6$ and $q=1.12$.

and approximate analytical forms in the first finite band gap of the model's linear spectrum. The analytical approximation based on the VA (variational approximation) for the soliton's shape and balance equation for the total power yields results which turn out to be quite accurate in comparison with the numerical findings (for the fundamental and vortical solitons alike), except for the fact that the analytical approximation underestimates the region of the existence of stable DGSs. The model considered in this work can be realized as a laser cavity in a bulk self-defocusing optical waveguide equipped with a transverse grating.

The analysis of the model can be developed in other directions. In particular, it may be interesting to construct solitary vortices with multiple values of the topological charge (stable 2D gap solitons with embedded vorticity 2 were found in the conservative model). A challenging problem is to find DGSs and vortices in higher finite band gaps of the underlying linear spectrum.

[1] I. S. Aranson and L. Kramer, Rev. Mod. Phys. **74**, 99 (2002); *Dissipative Solitons*, edited by N. Akhmediev and A. Ankiewicz (Springer-Verlag, Berlin, Heidelberg, 2005); B. A. Malomed, in *Encyclopedia of Nonlinear Science*, edited by A. Scott (Routledge, New York, 2005), p. 157.

[2] F. T. Arecchi, S. Boccaletti, and P. Ramazza, Phys. Rep. **318**, 1 (1999); P. Mandel and M. Tlidi, J. Opt. B: Quantum Semiclassical Opt. **6**, R60 (2004); N. N. Rosanov, S. V. Fedorov, and A. N. Shatsev, Appl. Phys. B: Lasers Opt. **81**, 937 (2005).

[3] M. E. Fermann, A. Galvanauskas, G. Sucha, and D. Harter, Appl. Phys. B: Lasers Opt. **65**, 259 (1997); M. F. S. Ferreira, M. M. V. Facao, and S. C. V. Latas, Fiber Integr. Opt. **19**, 31 (2000); F. O. Ilday and F. W. Wise, J. Opt. Soc. Am. B **19**, 470 (2002); Y. D. Gong, P. Shum, D. Y. Tang, C. Lu, X. Guo, V. Paulose, W. S. Man, and H. Y. Tam, Opt. Laser Technol. **36**, 299 (2004); W. H. Renninger, A. Chong, and F. W. Wise, Phys. Rev. A **77**, 023814 (2008).

[4] J. N. Kutz, SIAM Rev. **48**, 629 (2006).

[5] P. Kolodner, Phys. Rev. Lett. **66**, 1165 (1991); Phys. Rev. A **43**, 2827 (1991); **44**, 6448 (1991); **44**, 6466 (1991); J. A. Glazier and P. Kolodner, *ibid.* **43**, 4269 (1991).

[6] L. M. Hocking and K. Stewartson, Proc. R. Soc. London, Ser. A **326**, 289 (1972); N. R. Pereira and L. Stenflo, Phys. Fluids **20**, 1733 (1977).

[7] B. A. Malomed, M. Goelles, I. M. Uzunov, and F. Lederer, Phys. Scr. **55**, 73 (1997).

[8] V. I. Petviashvili and A. M. Sergeev, Dokl. Akad. Nauk SSSR **276**, 1380 (1984) [Sov. Phys. Dokl. **29**, 493 (1984)].

[9] B. A. Malomed, Physica D **29**, 155 (1987).

[10] O. Thual and S. Fauve, J. Phys. (France) **49**, 1829 (1988); S. Fauve and O. Thual, Phys. Rev. Lett. **64**, 282 (1990); W. van Saarloos and P. C. Hohenberg, *ibid.* **64**, 749 (1990); B. A. Malomed and A. A. Nepomnyashchy, Phys. Rev. A **42**, 6009 (1990); V. Hakim, P. Jakobsen, and Y. Pomeau, Europhys. Lett. **11**, 19 (1990); P. Marcq, H. Chaté, and R. Conte, Physica D **73**, 305 (1994); J. M. Soto-Crespo, N. N. Akhmediev, and V. V. Afanasjev, J. Opt. Soc. Am. B **13**, 1439 (1996); O. Descalzi, M. Argentina and E. Tirapegui, Phys. Rev. E **67**, 015601(R) (2003); H. Sakaguchi, Physica D **210**, 138 (2005).

[11] A. Sigler and B. A. Malomed, Physica D **212**, 305 (2005); A. Sigler, B. A. Malomed, and D. V. Skryabin, Phys. Rev. E **74**, 066604 (2006).

[12] H. Sakaguchi and H. R. Brand, Physica D **117**, 95 (1998).

[13] W. Chen and D. L. Mills, Phys. Rev. Lett. **58**, 160 (1987); D. L. Mills and S. E. Trullinger, Phys. Rev. B **36**, 947 (1987).

[14] D. N. Christodoulides and R. I. Joseph, Phys. Rev. Lett. **62**, 1746 (1989); A. B. Aceves and S. Wabnitz, Phys. Lett. A **141**, 37 (1989).

[15] C. M. de Sterke and J. E. Sipe, Prog. Opt. **33**, 203 (1994).

[16] O. Zobay, S. Pötting, P. Meystre, and E. M. Wright, Phys. Rev. A **59**, 643 (1999); F. Kh. Abdullaev, B. B. Baizakov, S. A. Darmanyan, V. V. Konotop, and M. Salerno, *ibid.* **64**, 043606 (2001); A. Trombettoni and A. Smerzi, Phys. Rev. Lett. **86**, 2353 (2001); G. L. Alfimov, V. V. Konotop, and M. Salerno, Europhys. Lett. **58**, 7 (2002).

[17] H. Sakaguchi and B. A. Malomed, J. Phys. B **37**, 1443 (2004).

[18] B. B. Baizakov, V. V. Konotop, and M. Salerno, J. Phys. B **35**, 5105 (2002).

[19] P. J. Y. Louis, E. A. Ostrovskaya, C. M. Savage, and Y. S. Kivshar, Phys. Rev. A **67**, 013602 (2003); E. A. Ostrovskaya and Y. S. Kivshar, Opt. Express **12**, 19 (2004); H. Sakaguchi and B. A. Malomed, J. Phys. B **37**, 2225 (2004).

[20] E. A. Ostrovskaya and Y. S. Kivshar, Phys. Rev. Lett. **93**, 160405 (2004); E. A. Ostrovskaya, T. J. Alexander, and Y. S. Kivshar, Phys. Rev. A **74**, 023605 (2006); A. Gubeskys and B. A. Malomed, Phys. Rev. A **76**, 043623 (2007).

[21] B. J. Eggleton, R. E. Slusher, C. M. de Sterke, P. A. Krug, and J. E. Sipe, Phys. Rev. Lett. **76**, 1627 (1996); B. J. Eggleton, C. M. de Sterke, and R. E. Slusher, J. Opt. Soc. Am. B **16**, 587 (1999); J. T. Mok, C. M. de Sterke, I. C. M. Litter, and B. J. Eggleton, Nat. Phys. **2**, 775 (2006).

[22] B. Eiermann, Th. Anker, M. Albiez, M. Taglieber, P. Treutlein, K.-P. Marzlin, and M. K. Oberthaler, Phys. Rev. Lett. **92**, 230401 (2004); O. Morsch and M. Oberthaler, Rev. Mod. Phys. **78**, 179 (2006).

[23] H. Sakaguchi and B. A. Malomed, Phys. Rev. E **77**, 056606 (2008).

[24] N. K. Efremidis, S. Sears, D. N. Christodoulides, J. W. Fleischer, and M. Segev, Phys. Rev. E **66**, 046602 (2002); J. W. Fleischer, T. Carmon, M. Segev, N. K. Efremidis, and D. N. Christodoulides, Phys. Rev. Lett. **90**, 023902 (2003); F. Chen, M. Stepić, C. E. Rüter, D. Runde, D. Kip, V. Shandarov, O. Manela, and M. Segev, Opt. Express **13**, 4314 (2005).

[25] F. X. Kärtner and U. Keller, Opt. Lett. **20**, 16 (1995); J. N. Kutz, B. C. Collins, K. Bergman, S. Tsuda, S. Cundiff, W. H. Knox, P. Holmes, and M. Weinstein, J. Opt. Soc. Am. B **14**, 2681 (1997).

[26] X. Tr. Tran and , N. N. Rosanov, Opt. Spektrosk. **101**, 286 (2006) [Opt. Spectrosc. **101**, 271 (2006)]; N. N. Rosanov and Tr. X. Tran, Opt. Spektrosk. **105**, 432 (2008) [Opt. Spectrosc. **105**, 393 (2008)].

[27] N. N. Rosanov and Tr. X. Tran, Chaos **17**, 037114 (2007).

[28] B. B. Baizakov, B. A. Malomed, and M. Salerno, Europhys. Lett. **63**, 642 (2003).

[29] A. Gubeskys, B. A. Malomed, and I. M. Merhasin, Stud. Appl. Math. **115**, 255 (2005).

[30] H. Sakaguchi and B. A. Malomed, Phys. Rev. A **79**, 043606 (2009).

[31] S. K. Adhikari and B. A. Malomed, Phys. Rev. A **77**, 023607 (2008).